



## Induction of oxidative stress and DNA damage in human renal proximal tubular cells by aristolochic acid

Follow this and additional works at: <https://www.jfda-online.com/journal>

### Recommended Citation

Yu, F.-Y.; Chu, T.-Y.; Lian, J.-D.; Wu, S.-W.; Hung, T.-W.; and Chang, H.-R. (2011) "Induction of oxidative stress and DNA damage in human renal proximal tubular cells by aristolochic acid," *Journal of Food and Drug Analysis*: Vol. 19 : Iss. 2 , Article 2.

Available at: <https://doi.org/10.38212/2224-6614.2231>

This Original Article is brought to you for free and open access by Journal of Food and Drug Analysis. It has been accepted for inclusion in Journal of Food and Drug Analysis by an authorized editor of Journal of Food and Drug Analysis.

# Induction of Oxidative Stress and DNA Damage in Human Renal Proximal Tubular Cells by Aristolochic Acid

FENG-YIH YU<sup>1,2</sup>, TING-YEN CHU<sup>1,3</sup>, JONG-DA LIAN<sup>4</sup>, SHENG-WEN WU<sup>3,4</sup>,  
TUNG-WEI HUNG<sup>3,4</sup> AND HORNG-RONG CHANG<sup>3,4\*</sup>

<sup>1</sup>. Department of Biomedical Sciences, Chung Shan Medical University, Taichung, Taiwan, R.O.C.

<sup>2</sup>. Department of Medical Research, Chung Shan Medical University Hospital, Taichung, Taiwan, R.O.C.

<sup>3</sup>. Institute of Medicine, Chung Shan Medical University, Taichung, Taiwan, R.O.C.

<sup>4</sup>. Division of Nephrology, Department of Internal Medicine, Chung Shan Medical University Hospital, Taichung, Taiwan, R.O.C.

(Received: September 10, 2010; Accepted: March 4, 2011)

## ABSTRACT

Aristolochic acid I (AAI) is found primarily in the plant *Aristolochia*. Consumption of products containing AAI has been linked with permanent kidney damage and urothelial carcinoma. This study applied human proximal tubule epithelial cell line (HK-2) to examine the relationship among AAI-induced intracellular oxidative stress, DNA damage and MAP kinase activation. High concentrations of AAI caused a decrease in cell viability and an increase in the activity of caspase 3. AAI treatment also led to a dose-dependent increase of reactive oxygen species (ROS) in HK-2 cells, and the presence of antioxidant glutathione (GSH) effectively inhibited ROS generation. Stimulating HK-2 cultures with AAI also led to GSH depletion. Results from single cell gel electrophoresis (SCGE) assays demonstrated that AAI showed the ability to increase the levels of DNA strand breaks in HK-2 cells. Up-regulation of luciferase activity driven by the Nrf2 binding element was also observed after 200  $\mu$ M AAI treatment. Exposure of HK-2 cells with AAI activated both ERK1/2 and p38 kinase phosphorylation, while only the MEK1/2 inhibitor, U0126, significantly decreased the levels of AAI-mediated ROS. In addition, both U0126 and SB202190 effectively reversed the levels of DNA damage triggered by AAI. This suggests that AAI treatment of HK-2 results in ROS formation and DNA damage. Furthermore, ROS generation occurs via the MEK/ERK1/2 signaling pathway, whereas DNA damage occurs via both the ERK1/2 and p38 pathways.

Key words: aristolochic acid, reactive oxygen species, DNA damage

## INTRODUCTION

Aristolochic acid (AA) is a nitrophenanthrene derivative isolated from the roots of the plant *Aristolochia clematitidis* and has been shown to be a nephrotoxic compound<sup>(1)</sup> and genotoxic mutagen<sup>(2-3)</sup>. Clinically, rapidly progressive renal fibrosis occurs after weight-reducing regimen including Chinese herbs containing AA has been identified as AA nephropathy<sup>(4)</sup>. Several clinical presentations have been described in Taiwan<sup>(5)</sup>, UK<sup>(6)</sup>, France<sup>(7)</sup> and Spain<sup>(8)</sup>, and currently AA nephropathy is a problem worldwide<sup>(1)</sup>.

Many studies<sup>(9-11)</sup> have been conducted involving the mutagenic and carcinogenic properties of AA, focusing on the formation of AA DNA adducts, activation of Ha-ras oncogene and overexpression of p53. In the renal and urethral tissue of the patients with AA nephropathy, three AA-specific DNA adducts, including one major (dA-AAI) and two minor

adducts (dG-AAI and dA-AAII), have been identified<sup>(9-10)</sup>. The major adenine adduct of AAI, dA-AAI, is detectable at relatively high levels in native kidney tissue up to 89 months after patients stopped taking the herbal medicine<sup>(9)</sup>. Furthermore, the dA-AAI adduct was also highly persistent in the kidneys of rats<sup>(11)</sup>.

Recently, Liu *et al.* examined the effect of AAI on renal tubular epithelial Madin-Darby canine kidney (MDCK) cells. Significant apoptosis was observed with AAI at as low as 25  $\mu$ M, following exposure for 24 h. In addition, the levels of reactive oxygen species (ROS) were increased following treatment with AAI at concentrations of 5, 25 and 25  $\mu$ M, respectively, for 4 h<sup>(12)</sup>. Administration of AA to Wistar rats for 5 days leads to oxidative stress, active caspase-3 expression, and mitochondrial injury within tubular cells<sup>(13)</sup>. In addition, a rapidly growing amount of literature suggests that a transient increase in ROS levels is closely associated with various signaling molecules, including those in MAPK pathways<sup>(14,15)</sup>. Therefore, in the present study, human renal

\* Author for correspondence. Tel: +886-4-24739595 ext. 32630;  
Fax: +886-4-24739595 ext. 32624; E-mail: chrcsmu@yahoo.com.tw

tubular cell (HK-2) was used as a model to examine the relationships among AAI-induced oxidative stress, DNA damage and MAPK pathway activation.

## MATERIALS AND METHODS

### I. Reagents

Pure AAI (Cat. No. 5512) was purchased from Sigma Chemical Co. (St. Louis, MO, USA). Cell culture medium and serum were obtained from Life Technologies (Grand Island, NY, USA). Rabbit polyclonal antibodies against phospho-ERK1/2 (Thr202/Tyr204), ERK1/2, phospho-p38, p38 kinase, phospho-JNK/SAPK (Thr183/Tyr185) and JNK/SAPK were purchased from Cell Signaling (Beverly, MA, USA). Mouse monoclonal antibodies against  $\alpha$ -tubulin and  $\beta$ -actin were purchased from Sigma Chemical Co. U0126 (MEK1/2 Inhibitor), SB 203580 and SB202190 (p38 inhibitors) were purchased from Cell Signaling (Beverly, MA, USA). Horseradish peroxidase-conjugated goat anti-rabbit/mouse IgG secondary antibodies were obtained from Pierce (Rockford, IL, USA).

### II. Cell Culture

Human renal proximal tubular epithelial cell line (HK-2) was obtained from the Bioresources Collection and Research Center in Taiwan. HK-2 cells were maintained in DMEM/Hams F12 supplemented with 10% fetal bovine serum, 100 U/mL of penicillin and 0.1 mg/mL of streptomycin at 37°C in a humidified 5% CO<sub>2</sub> incubator.

### III. Cell Viability Assay

HK-2 cells ( $8 \times 10^3$  cells) were seeded in 96-well plates, treated with vehicle alone (25% ethanol in PBS) or various concentrations (50 - 200  $\mu$ M) of AA at designated times. MTT (3-(4,5-Dimethylthiazol-2-yl)-2,5-diphenyltetrazolium bromide) assay, a method applying the mitochondrial metabolic enzyme activity as an indicator of cell viability, was conducted following the protocol described in the report of Liu *et al.*<sup>(16)</sup>

### IV. Measurement of Caspase-3 Activity

Caspase-3 activity was determined according to the principle of Gurtu *et al.*<sup>(17)</sup> Cells in 35-mm plates ( $2 \times 10^5$  cells/well) were incubated with vehicle or various concentrations of AA for 24 h. Treated cells were washed with 0.01 N of PBS and resuspended in 100  $\mu$ L of assay buffer containing 0.1 M of HEPES (pH 7.4), 2 mM of DTT, 1% sucrose and 0.1% CHAPS. The cell suspension was sonicated and centrifuged ( $14,000 \times g$ ) at 4°C for 15 min before the addition of 20  $\mu$ M of Ac-DEVD-AFC (Sigma), a substrate for active caspase-3 protein. After incubation at 37°C for 1 h, the levels of cleaved products were measured using a HTS 7000 PLUS bioassay

reader (Perkin Elmer, Boston, MA, USA) with excitation set at 405 nm and emission at 535 nm.

### V. Measurement of ROS Levels

ROS levels were determined based on Kim *et al.*<sup>(18)</sup> with a slight modification. HK-2 cells ( $8 \times 10^3$ /per well on a 96-well tissue culture plate) were cultured for at least 18 h in 50  $\mu$ L of complete medium, and then 50  $\mu$ L of H<sub>2</sub>DCF-DA (20  $\mu$ M) in Krebs-Ringer HEPES (KRH) buffer was added. Thirty minutes after incubation, the probe-containing medium was removed and various concentrations of AAI in medium were added and incubated for another 18 h at 37°C. For the experiments using inhibitors, after H<sub>2</sub>DCF-DA-containing medium was removed, antioxidant or MAPK inhibitors were added 2 h before co-incubation with AAI for another 18 h. Since H<sub>2</sub>DCF-DA is hydrolyzed and oxidized by intracellular ROS to 2,7-dichlorofluorescein (DCF), the fluorescence of DCF was analyzed in an HTS 7000 Bio Assay Fluorescent Plate Reader (Perkin Elmer Life Sciences) at an excitation wavelength of 485 nm and emission at 530 nm.

### VI. GSH Level Determination

HK-2 cells ( $2.5 \times 10^5$ ) were plated in a 35-mm petri dish overnight, prior to experimental manipulation. The cultures were treated with solvent or AAI for 1 h and then washed with PBS followed by disrupting the cells in 200 mL of ice-cold distilled sterilized water containing 30 mM of EDTA. Cell lyses after centrifugation at  $10,000 \times g$  for 15 min were mixed with the freshly prepared GSH assay reagent (16.6% of 0.1% *O*-phthalaldehyde in methanol and 83.4% of 0.1 M sodium phosphate buffer (pH 8.0)) at a ratio of 3 : 10. The mixtures were maintained in darkness at room temperature for 15 min and then the GSH-*O*-phthalaldehyde derivative was detected with fluorescence (excitation/emission: 350/420 nm) by a fluorescence spectrophotometer (Molecular Devices, Sunnyvale, CA, USA)

### VII. Single Cell Gel Electrophoresis Assay (Comet Assay)

A comet assay was conducted based on the principle of Tice *et al.*<sup>(19)</sup> Briefly, HK-2 cells ( $2 \times 10^5$  in a 35-mm plate) were cultured in a medium containing vehicle alone or various concentrations of AAI for 24 h. The adherent cells were then trypsinized and mixed with 1% low-melting-point agarose at 42°C. The mixtures were immediately transferred to the CometSlide™ (Trevigen Inc., Gaithersburg, MD) and the slides were immersed in ice-cold lysis solution (2.5 M of NaCl, 100 mM of EDTA (pH 10), 10 mM of Tris, 1% sodium lauryl sarcosinate, 1% Triton X-100, and 1% DMSO) for 1 h. After electrophoresis in an alkaline buffer (300 mM of NaOH, 1 mM of EDTA, pH > 13) at 300 mA for 30 min, DNA on the slides was stained with SYBR green I. The image of each cell on the slides was visualized and photographed under a fluorescence microscope (Axiovert 25, Zeiss). Each image was analyzed with the computer software from Euclid

Analysis (St. Louis, MO, USA) to calculate the tail moment, a combination of the amount of DNA in the tail with the distance of migration. For each independent experiment, the DNA damage levels of 80 individual cells were measured from each culture.

### IX. Western Blot Analysis

HK-2 cells at 80% confluence were pretreated with or without MAPK inhibitors (20  $\mu$ M of U0126/ 20  $\mu$ M of SB203580/ 20  $\mu$ M of SB202190) for 30 min, before co-exposure to AAI for another 24 h. Whole cell extracts were prepared according to Liu *et al.*<sup>(16)</sup> and the protein concentrations were determined using Bradford protein assay (Bio-Rad, Hercules, CA, USA). Equal amounts of proteins (40  $\mu$ g) from each sample were separated by 10% SDS-polyacrylamide gel electrophoresis. The proteins were transferred to nitrocellulose membranes (Bio-Rad, Hercules, CA, USA), and reacted with primary antibodies specific to MAPKs (phospho-ERK1/2, ERK1/2, phospho-p38 kinase, p-38 kinase, phospho-JNK and JNK) for 12 h at 4°C and then with anti-rabbit secondary antibodies conjugated to horseradish peroxidase for another 1 h at room temperature. Bound antibodies on the membrane were detected using an enhanced chemiluminescence detection system according to the manufacturer's manual (Amersham Pharmacia Biotech, Amersham, UK). The intensities of bands on the blots were quantitated by densitometric analysis using ImageGauge software Ver. 3.46 (Fuji Photo Film, Tokyo, Japan). The relative phospho-ERK/ERK and phospho-p38/p38 ratios were determined by the intensities obtained from three independent experiments.

### X. Transfection

HK-2 cells, grown in 3.5-cm culture plates with serum free medium, were 70 - 80% confluence at the time of transfection. Cells were co-transfected with 2  $\mu$ g of p2xARE/Luc and 1  $\mu$ g of pSV- $\beta$ -galactosidase control vector (Promega, Madison, WI, USA) with Lipofectamine 2000 (Invitrogen, Carlsbad, CA, USA) according to the manufacturer's recommendations. The plasmid p2xARE/Luc with two binding sites (5'-TGACTCAGCA-3') of nuclear factor-erythroid 2 p45-related factor 2 (Nrf2) was kindly provided by Dr. Being-Sun Wung at National Chiayi University<sup>(20)</sup>. Consequently, the transfected cells were incubated in the CO<sub>2</sub> incubator for 6 h prior to replacement with fresh medium containing 10% bovine serum. Eighteen hours after medium replacement, the transfected cells were exposed to solvent or various concentrations of AAI for 24 h before determination of intracellular luciferase activity.

### XI. Luciferase Reporter Assay

The total protein extracts from AAI-treated cultures were prepared by lysing the cells with 1x lysis reagent containing 25 mM of Tris-phosphate (pH 7.8), 2 mM of DTT,

2 mM of 1, 2-diamino cyclohexane-N', N', N', N'-tetraacetic acid, 10% glycerol, and 1% Triton X-100. The supernatant fluid after centrifugation (5 min at 10,000  $\times$ g) was divided into two parts. One fraction was subjected to luciferase assay kit (Promega, Madison, WI, USA) and Tropic TR717 luminometer (Applied Biosystems, Foster city, CA, USA) according to the manufacturer's instructions. The other part is for  $\beta$ -galactosidase activity determination; protein extracts were added into an equal volume of 2 $\times$  assay buffer [substrate ONPG (O-nitrophenyl-d-galactopyranoside) 1.33 mg/mL, 200 mM of sodium phosphate buffer (pH 7.3), 2 mM of MgCl<sub>2</sub> and 100 mM of  $\beta$ -mercaptoethanol] and then the mixtures were incubated at 37°C for 30 min. The reaction was terminated by addition of sodium carbonate and the absorbance was read at 420 nm with an Optimax microplate reader (Molecular Device, CA, USA). To account for the differences in transfection rates, the data of luciferase activity were normalized to the  $\beta$ -galactosidase activity.

### XII. Statistical Analysis

Data were expressed as mean and SEM (standard error of mean). All statistical analyses were conducted using the software GraphPad Prism Version 4.0 (GraphPad Software, San Diego, CA, USA). Experimental data grouped by one variable were analyzed by unpaired two-tailed t-test or one-way ANOVA followed by Tukey post test.

## RESULTS

### I. AAI Decreased Cell Viability and Increased Caspase-3 Activity of HK-2 Cells

To determine the AAI concentrations suitable for studying ROS formation, the cell viability of HK-2 treated with vehicle or AAI was examined by the tetrazolium dye-based MTT assay. At a concentration of 200  $\mu$ M, the cell viability declined to 85% of control after 24 h exposure (Figure 1A); however, no significant cell viability difference was observed when HK-2 cells were exposed for 1 h to AAI at concentrations up to 500  $\mu$ M (data not shown). Furthermore, treatment of HK-2 cells with concentrations of 100  $\mu$ M or greater caused a significant increase in caspase-3 catalytic activity (Figure 1B). These data suggest that apoptosis contributes partially to AAI-induced cytotoxicity.

### II. AAI Induced ROS Formation and GSH Depletion in HK-2 Cells

The ROS level in AAI-treated HK-2 cells was evaluated using fluorescent dye H<sub>2</sub>DCF-DA as the oxidant-reacting probe. Following treatment of HK-2 cells with various concentrations of AAI for 1 h, intracellular fluorescence level increased in a dose-dependent pattern; AAI at 100 and 200  $\mu$ M increased fluorescence to 1.8 and 3.5 folds of control levels, respectively (Figure 2A). In addition, when cells were

pre-exposed to free radical scavengers, including Tiron, NAC, or GSH, before co-incubation with AAI, only GSH showed significant inhibitory effect on the AAI-induced ROS formation (Figure 2B).

We further investigated the role of GSH in AAI-induced ROS, since the intracellular GSH level is generally considered to be closely correlated with ROS generation. HK-2 cells were treated with solvent or AAI for 1 h before determination of the total GSH content. The GSH level significantly dropped to 73% of the control group in 500  $\mu\text{M}$ -AAI exposed cultures (Figure 2C), revealing that AAI may induce GSH depletion which contributes to ROS generation.

### III. AAI Treatment Led to DNA Damage of HK2 Cells

To investigate whether AAI-stimulated ROS contributed to oxidative DNA damage, single cell gel electrophoresis (SCGE) assay (also named comet assay), in which data were collected on a single cell base, was applied. The value of tail moment indicates the direct strand breaks and/or alkaliabile

site generation on the chromosome<sup>(21)</sup>. Exposure of HK-2 to 100  $\mu\text{M}$  of AAI led to the formation of a “comet tail”, as shown in Figure 3A. Furthermore, administering various concentrations of AAI resulted in a concentration-dependent increase in the tail moment values (Figure 3B). The tail moment values at AAI concentrations of 50  $\mu\text{M}$  and 200  $\mu\text{M}$  elevated to 3.9 and 6.3 folds of the control, respectively. However, preincubation

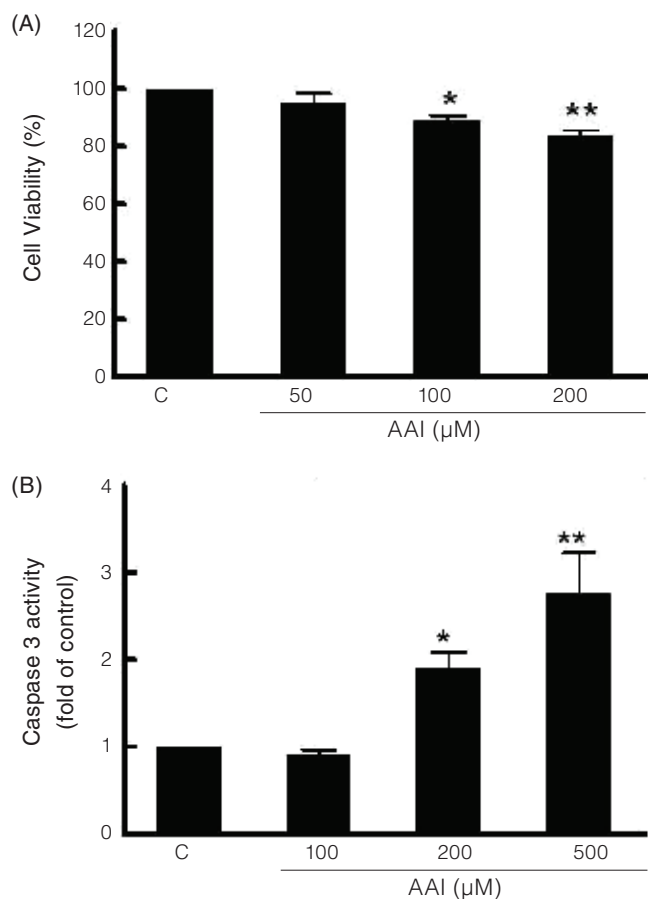


**Figure 1.** AAI decreased cell viability and increased caspase-3 activity of HK-2 cells. HK-2 cells were treated with vehicle or AAI for 24 h. (A) The cell viability was determined by MTT assay. (B) Total cellular proteins were extracted and caspase-3 activity was measured as described in the Materials and Methods section. The data from three independent experiments are expressed as the mean  $\pm$  SEM. \* Significant difference ( $*p < 0.05$ ;  $**p < 0.01$ ) compared to the solvent-treated control.

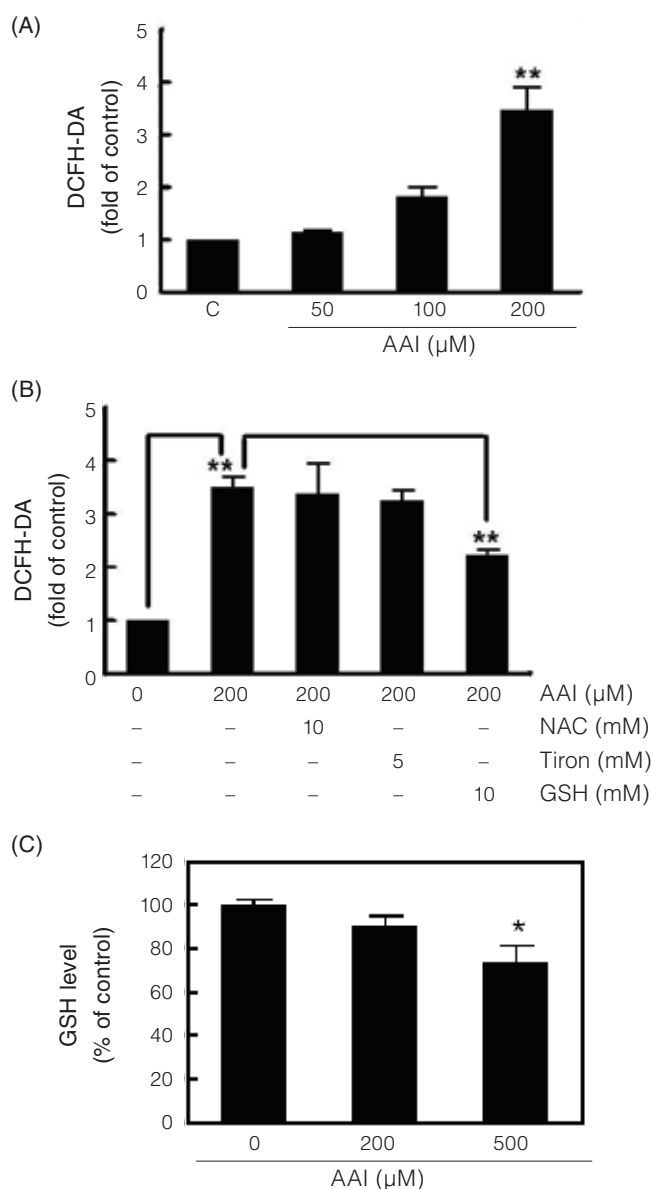


**Figure 2.** AAI induced ROS formation and GSH depletion in HK-2. (A) HK-2 cells were incubated with 10  $\mu\text{M}$  of  $\text{H}_2\text{DCFH-DA}$  for 30 min, and then the medium was replaced with solvent or various concentrations of AAI for 18 h or (B) HK-2 cells were pre-treated with or without NAC (10 mM), Tiron (5 mM), or GSH (10 mM) for 2 h and then incubated with or without AAI (200  $\mu\text{M}$ ) for another 18 h. DCF fluorescence was measured by fluorocytometry. (C) HK-2 cells were exposed to solvent or AAI for 1 h before determination of the GSH level according to the Materials and Methods section. All the data are expressed as the mean  $\pm$  SEM from at least three independent experiments. \* Significant difference compared to the solvent-treated control or the paired group.

of HK-2 cells with various antioxidants, including NAC, Tiron or GSH, did not show any effect on prevention of AAI-induced DNA damage (data not shown).

To correspond to ROS generation and associated DNA damage, antioxidant genes may be activated to diminish the ROS generation caused by environment stimuli. Among these antioxidant response, transcription factor Nrf2 works as a master regulator and binds to the antioxidant response element (ARE) in the upstream promoter region of many antioxidative genes<sup>(22-23)</sup>. Therefore, HK-2 cells were transiently transfected with pARE/Luc before exposed to AAI for 24 h. As shown in Figure 4A, AAI at a concentration of 200  $\mu$ M was able to up-regulate the level of luciferase reporter activity in HK-2 cells, suggesting that after induction of ROS formation by AAI, antioxidant genes with Nrf2 binding site in the promoter regions may be activated. Therefore, we further examined the expression level of the HO-1 gene, which is known to be induced by oxidants in mammalian cells<sup>(24)</sup> and has a predicted Nrf2 binding site on its promoter<sup>(23)</sup>. Western blotting demonstrated that

HO-1 protein was not detected in AAI-stimulated cultures, but the signal was highly up-regulated by sodium arsenite ( $\text{NaAsO}_2$ ), a positive control (Figure 4B).

#### IV. ERK1/2 Played a Role in AAI-Triggered ROS

It has been shown that oxidative stress caused by stimuli may be associated with MAPK signaling pathways<sup>(14)</sup>. Therefore, we evaluated whether AAI can activate MAPK pathways in HK-2 cells. Exposure of cells to 200  $\mu$ M of AAI resulted in both ERK1/2 and p38 phosphorylation (Figure 5), but not JNK pathway (data not shown). In addition, the presence of GSH did not affect the activation of ERK1/2 or p38. The presence of U0126, a specific MEK1/2 inhibitor, significantly down-regulated the signal of phospho-ERK1/2 induced by 200  $\mu$ M of AAI (Figure 6A). Furthermore, U0126 dramatically decreased the ROS level stimulated by AAI. However, preincubation of cells with either SB203580 or SB202190, two p38 pathway blockers, did not show any substantial effect on ROS level (Figure 6B), indicating that ERK1/2 signaling, but not the p38 pathway, partially contributes to AAI-induced ROS generation.

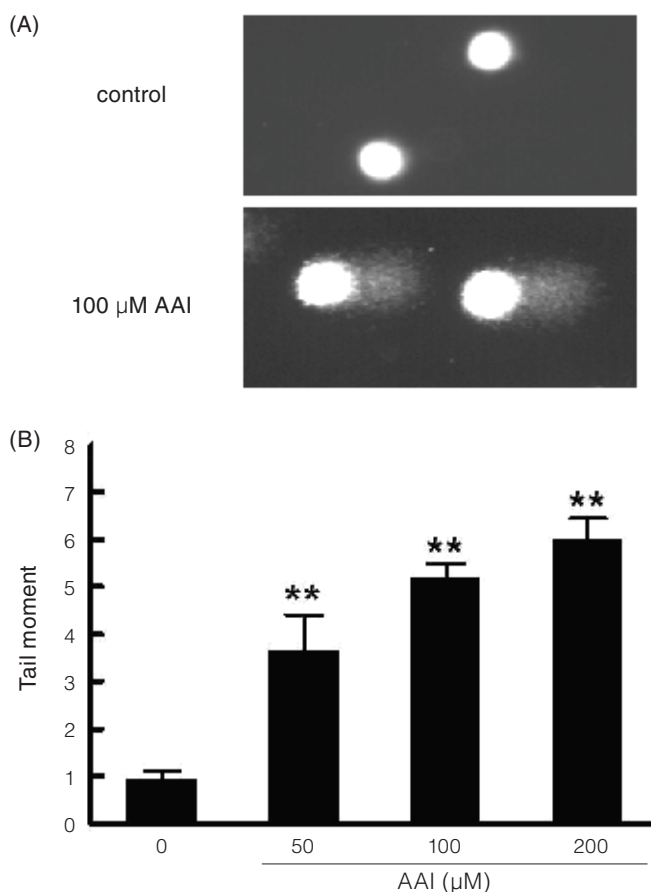


**Figure 3.** AAI induced DNA damage in HK2 cells. HK-2 cells were treated with solvent (control) or various concentrations of AAI for 24 h. Treated cells were subjected to a comet assay and the images from fluorescence microscopy are shown in (A). (B) The densities of cell images and the tail moment values were analyzed and calculated using computer software. All the data are expressed as the mean  $\pm$  SEM from four independent experiments. \* Significant difference (\*\*  $p < 0.01$ ) compared to the solvent-treated control.

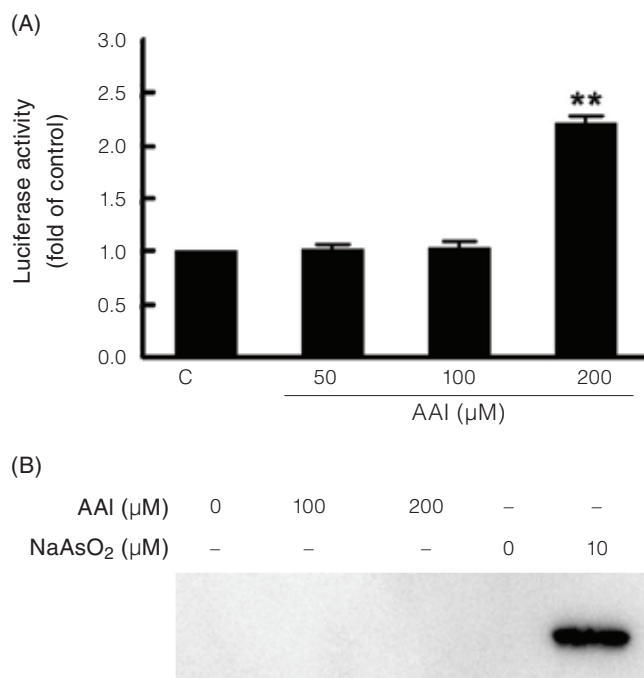


**Figure 4.** (A) AAI increased the luciferase activity of Nrf2 binding element. HK-2 cells were transiently co-transfected with p2xARE/Luc and  $\beta$ -galactosidase plasmids, and then incubated with solvent or various concentrations of AAI for 24 h. The cells were lysed and analyzed for luciferase and galactosidase activities as described in the Material and Methods section. The result is an increased luciferase activity which has been normalized to the constitutively expressed  $\beta$ -galactosidase activity. Data are expressed as the mean  $\pm$  SEM from at least three independent experiments. (B) AAI did not induce the expression of the HO-1 gene. HK-2 cells were treated with solvent, AAI or  $\text{NaAsO}_2$  for 24 h and then the level of HO-1 protein was analyzed by Western blotting using antibodies specific to HO-1.

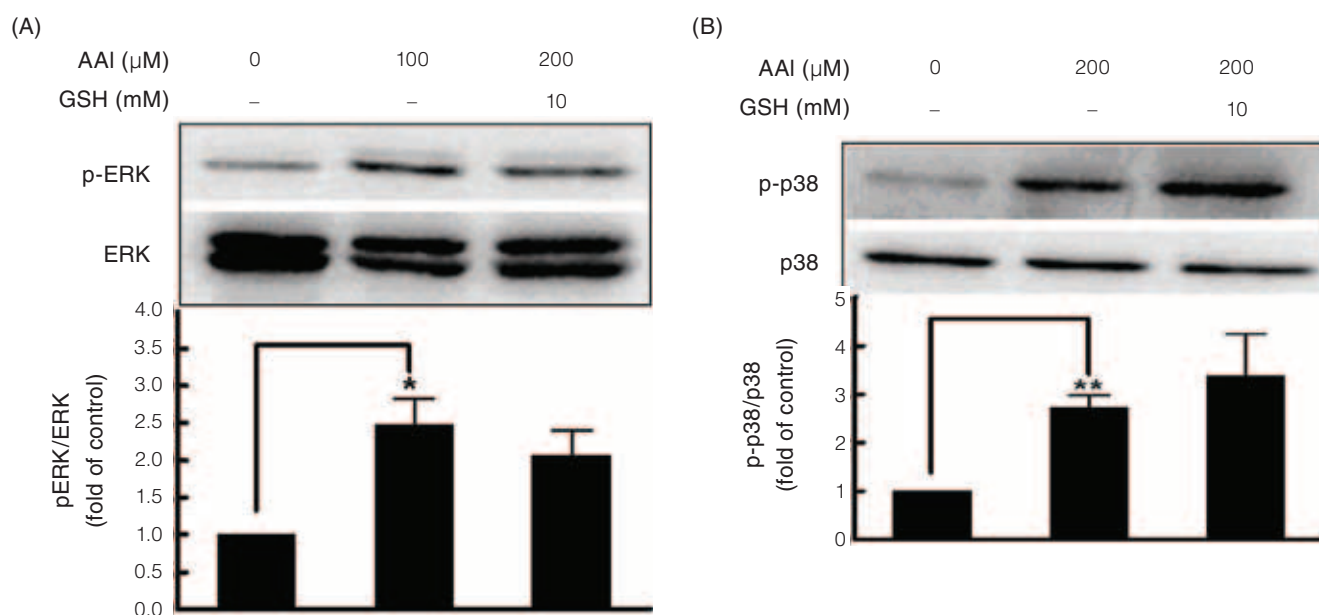


**Figure 5.** Effect of AAI on ERK1/2 and p38 phosphorylation. HK-2 cells were treated with or without GSH for 2 h before co-incubation with 200  $\mu\text{M}$  of AAI for another 24 h. MAPK activation was estimated by Western blotting using antibodies that recognize (A) phosphorylated/parent forms of ERK1/2 or (B) phosphorylated/parent forms of p38. The relative phospho-ERK/ERK and phospho-p38/p38 ratios were determined by densitometric analyses of three independent experiments and expressed as the mean  $\pm$  SEM. \* Significant difference ( $*p < 0.05$ ,  $**p < 0.01$ ) compared to the paired group.

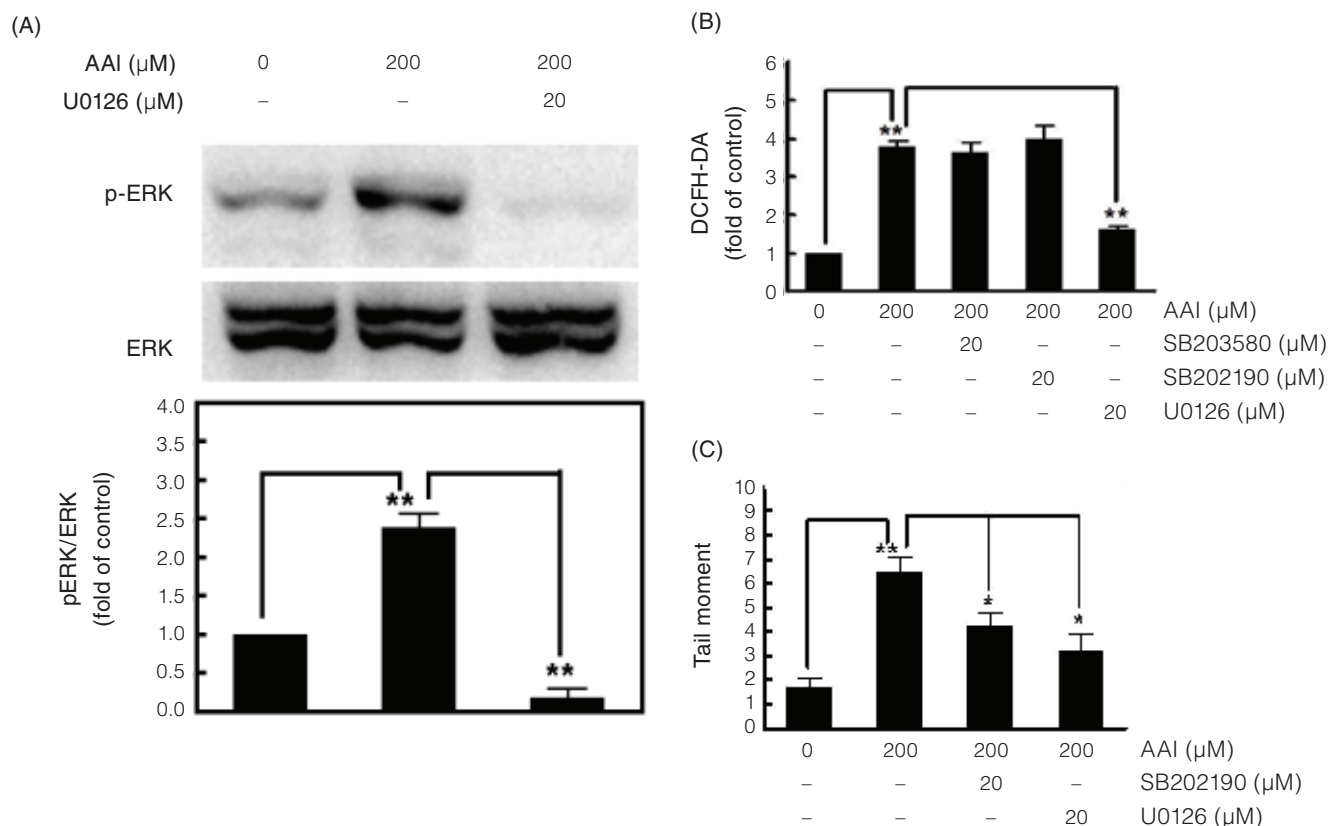


**Figure 6.** Effects of MAPK inhibitors on AAI-induced ROS and DNA damage. (A) HK-2 cells were pretreated with U0126 (MEK1/2 inhibitor) for 1 h and then co-incubated with solvent or 200  $\mu\text{M}$  of AAI for another 18 h. Western blotting was conducted using antibodies specific to phosphorylated/parent forms of ERK1/2. The relative phospho-ERK/ERK ratio was determined by densitometric analysis of three independent experiments. (B) HK-2 cells were pretreated with p38 kinase inhibitors (SB203580/SB202190) or U0126 for 1 h and then co-incubated with AAI for another 18 h for ROS determination, or (C) co-incubated with AAI for another 24 h for DNA damage analysis by Comet assay and the images from fluorescence microscope were analyzed with the computer software to calculate tail moment values. All the data are expressed as the mean  $\pm$  SEM from at least three independent experiments. \* Significant difference ( $**p < 0.01$ ) compared to the paired group.

### V. Both ERK1/2 and p38 Pathways Involved in AAI-triggered DNA Damage

To further investigate the role of MAPK in AAI-induced DNA damage, HK-2 cells were pretreated with SB202190 or U0126 for 1 h, and then co-exposed to AAI for another 24 h. The tail moment values of the treated cells were determined by Comet assay. Figure 6C demonstrated that AAI-induced DNA damage could be inhibited by either SB202190 or U0126, suggesting that both ERK1/2 and p38 signaling pathways are involved in AAI-induced DNA damage. Taking the aforementioned results together, a model for AAI-induced oxidative stress in HK-2 cells is proposed in Figure 7.

## DISCUSSION

AA, a mixture of AAI and AAI, is a natural component in herbal extracts of various *Aristolochia* species. Some of the *Aristolochia* species have been widely used in traditional Chinese medicine as anti-rheumatics, diuretics and in the treatment of oedema for thousands of years, but the components AAI and AAI are suspected to cause nephropathy in the past two decades<sup>(25)</sup>. Herbal remedies containing *Aristolochia* species have been classified to be carcinogenic to humans (Group 1) and the mixtures of AA are considered as probable carcinogens to humans (Group 2A)<sup>(26)</sup>. Most European countries and Taiwan have banned the use of certain *Aristolochia* species in herbal medicines. However, many commercialized products are still contaminated with AA because of misuse in drug preparation or confusion of close vernacular Chinese names<sup>(27)</sup>.

Our results provided evidence that AAI induces both ROS formation and DNA damage in HK-2 cells, which is consistent with the recent findings of Chen *et al.*<sup>(28)</sup> By subjecting the RNA from AA-treated HK-2 cells to microarray experiments, they observed that genes involved in DNA repair processes, DNA damage stimuli, and apoptosis were significantly regulated by AA treatment, suggesting that down-regulation of DNA repair gene expression is a possible mechanism for AA-induced genotoxicity. On the other hand, treatment of HK-2 cells with 200  $\mu$ M of AAI resulted in a significant increase in the luciferase activity of antioxidant response element (ARE) containing promoter (Figure 4A). Nrf2 is a transcription factor which binds to the ARE (also named Nrf2 binding site) in the promoter region of many anti-oxidative genes<sup>(22-23)</sup>. The HO-1 gene, which can be induced by many oxidants, such as hydrogen peroxide, heavy metals, ultraviolet radiation or sulfhydryl reagents, harbors a predicted Nrf2 binding site on its promoter. However, it was not successfully induced by the presence of AAI. This suggests that Nrf2 does not play a critical role in defending the oxidative stress stimulated by AAI. Chen *et al.*<sup>(28)</sup> also reported that the mRNA levels of two genes, GADD45B (growth arrest and DNA damage-inducible gene) and NAIP (NRL family-apoptosis inhibitory protein) were up-regulated corresponding to AA treatment. Using software for

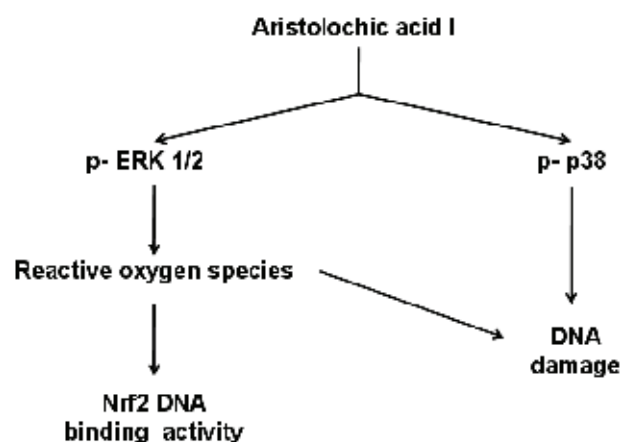


Figure 7. A proposed model for AAI-induced oxidative stress in HK-2 cells.

prediction, we found that the Nrf2 binding site was only found in the promoter region of GADD 45B, but not in that of the NAIP gen.

Adding GSH, but not NAC and Tiron, into HK-2 cultures effectively attenuated the ROS levels induced by AAI (Figure 2B). Furthermore, AAI stimulation resulted in the GSH depletion in HK-2 (Figure 2C), implying that GSH depletion may be the major factor contributing to AAI-induced oxidative stress. A similar phenomenon was also observed in AAI-treated HL-60 cultures; exposure of HL-60 to 200  $\mu$ M of AAI for 30 min led to the GSH level dropping to 55% of the control (data not shown). The intracellular GSH level is generally considered to be closely correlated with ROS generation<sup>(29)</sup>. Many studies have indicated that unstable ROS molecules after exposing to stimulators can be diminished by interacting with the cysteinyl moiety of GSH, and then the phenomenon of GSH depletion is subsequently observed. Since certain organic anion transporter in rats serves as a bidirectional transporter for the organic anion/GSH exchange, it is possible that AA induced-GSH depletion is mediated by GSH efflux through GSH/AA exchange<sup>(30-31)</sup>.

Treating HK-2 cells with 200  $\mu$ M of AAI activated both the phosphorylation of ERK1/2 and p38 MAP kinase (Figure 5A and 5B); both pathways were associated with the DNA damage caused by AAI (Figure 6B). However, AAI-induced ROS was selectively reduced by inhibition of the ERK1/2 pathway, but not p38 kinase (Figure 6A), indicating its dependence on MEK/ERK1/2 activation only. Several studies have mentioned that under certain circumstances, MEK/ERK1/2 signaling plays a pivotal role in ROS induction, but the exact molecular mechanism has not been fully elucidated<sup>(32,33)</sup>. Taken together, these results suggest that in addition to ROS, factors correlated with the p38 kinase pathway may also contribute to AAI-induced DNA damage. It is well known that the carcinogenic and mutagenic effects of AA are associated with the formation of AA-derived DNA adducts<sup>(34)</sup>. AAI has been found to bind covalently to the exocyclic amino group of purine nucleotides in DNA samples isolated from

patients with CHN<sup>(35)</sup>. Therefore, it is highly possible that the DNA damage shown in the SCGE assay resulted from both ROS attack and DNA adduct formation.

In summary, as shown in Figure 7, treatment of HK-2 with AAI resulted in the activation of ERK1/2 and p38 kinase pathways. The generation of DNA damage occurred via both the ERK1/2 and p38 pathways, whereas ROS generation occurred only through ERK1/2 cascade. High levels of ROS induced by AAI may also trigger an Nrf2-mediated antioxidant response.

### ACKNOWLEDGMENTS

This work was supported by grants NSC 95-2313-B-040-004 from the National Science Council of the Republic of China (Taiwan) and CSH-96-01 from Chung Shan University Hospital. Luminescent image analysis was performed in the Instrument Center of Chung Shan Medical University, which is supported by the National Science Council, Ministry of Education and Chung Shan Medical University.

### REFERENCES

1. Debelle, F. D., Vanherweghem, J. L., and Nortier, J. L. 2008. Aristolochic acid nephropathy: a worldwide problem. *Kidney Int.* 74: 158-169.
2. Arlt, V. M., Stiborova, M. and Schmeiser, H. H. 2002. Aristolochic acid as a probable human cancer hazard in herbal remedies: a review. *Mutagenesis* 17: 265-277.
3. Stemmer, K., Ellinger-Ziegelbauer, H., Ahr, H. J. and Dietrich, D. R. 2007. Carcinogen-specific gene expression profiles in short-term treated Eker and wild-type rats indicative of pathways involved in renal tumorigenesis. *Cancer Res.* 67: 4052-4068.
4. Vanherweghem, J. L., Depierreux, M., Tielemans, C., Abramowicz, D., Dratwa, M., Jadoul, M., Richard, C., Vandervelde, D., Verbeelen, D., Vanhaelen-Fastre, R. *et al.* 1993. Rapidly progressive interstitial renal fibrosis in young women: association with slimming regimen including Chinese herbs. *Lancet* 341: 387-391.
5. Yang, C. S., Lin, C. H., Chang, S. H., and Hsu, H. C. 2000. Rapidly progressive fibrosing interstitial nephritis associated with Chinese herbal drugs. *Am. J. Kidney Dis.* 35: 313-318.
6. Lord, G. M., Tagore, R., Cook, T., Gower, P. and Pusey, C. D. 1999. Nephropathy caused by Chinese herbs in the UK. *Lancet* 354: 481-482.
7. Stengel, B. and Jones, E. 1998. End-stage renal insufficiency associated with Chinese herbal consumption in France. *Nephrologie* 19: 15-20.
8. Pena, J. M., Borrás, M., Ramos, J. and Montoliu, J. 1996. Rapidly progressive interstitial renal fibrosis due to a chronic intake of a herb (*Aristolochia pistolochia*) infusion. *Nephrol. Dial. Transplant.* 11: 1359-1360.
9. Nortier, J. L., Martinez, M. C., Schmeiser, H. H., Arlt, V. M., Bieler, C. A., Petein, M., Depierreux, M. F., De Pauw, L., Abramowicz, D., Vereerstraeten, P. and Vanherweghem, J. L. 2000. Urothelial carcinoma associated with the use of a Chinese herb (*Aristolochia fangchi*). *N. Engl. J. Med.* 342:1686-1692.
10. Debelle, F. D., Nortier, J. L., De Prez, E. G., Garbar, C. H., Vienne, A. R., Salmon, I. J., Deschodt-Lanckman, M. M. and Vanherweghem, J. L. 2002. Aristolochic acids induce chronic renal failure with interstitial fibrosis in salt-depleted rats. *J. Am. Soc. Nephrol.* 13: 431-436.
11. Cosyns, J. P., Jadoul, M., Squifflet, J. P., Van Cangh, P. J. and van Ypersele de Strihou, C. 1994. Urothelial malignancy in nephropathy due to Chinese herbs. *Lancet* 344:188.
12. Liu, Q., Wang, Q., Yang, X., Shen, X. and Zhang, B. 2009. Differential cytotoxic effects of denitroaristolochic acid II and aristolochic acids on renal epithelial cells. *Toxicol. Lett.* 184: 5-12.
13. Pozdzik, A. A., Salmon, I. J., Debelle, F. D., Decaestecker, C., Van den Branden, C., Verbeelen, D., Deschodt-Lanckman, M. M., Vanherweghem, J. L. and Nortier, J. L. 2008. Aristolochic acid induces proximal tubule apoptosis and epithelial to mesenchymal transformation. *Kidney Int.* 73: 595-607.
14. McCubrey, J. A., Lahair, M. M. and Franklin, R. A. 2006. Reactive oxygen species-induced activation of the MAP kinase signaling pathways. *Antioxid. Redox. Sign.* 8: 1775-1789.
15. Matsuzawa, A. and Ichijo, H. 2008. Redox control of cell fate by MAP kinase: physiological roles of ASK1-MAP kinase pathway in stress signaling. *Biochim. Biophys. Acta* 1780: 1325-1336.
16. Liu, B. H., Wu, T. S., Yu, F. Y. and Wang, C. H. 2006. Mycotoxin patulin activates the p38 kinase and JNK signaling pathways in human embryonic kidney cells. *Toxicol. Sci.* 89: 423-430.
17. Gurtu, V., Kain, S. R., Zhang, G. 1997. Fluorometric and colorimetric detection of caspase activity associated with apoptosis. *Anal. Biochem.* 251: 98-102.
18. Kim, J. K., Pedram, A., Razandi, M. and Levin, E. R. 2006. Estrogen prevents cardiomyocyte apoptosis through inhibition of reactive oxygen species and differential regulation of p38 kinase isoforms. *J. Biol. Chem.* 281: 6760-6767.
19. Tice, R. R., Agurell, E., Anderson, D., Burlinson, B., Hatmann, A., Kobayashi, H., Miyamae, Y., Rojas, E., Ryu, J. C. and Sasaki, Y. F. 2000. Single cell gel/comet assay: guidelines for in vitro genetic toxicology testing. *Environ. Mol. Mutagen.* 35: 206-221.
20. Liao, B. C., Hsieh, C. W., Liu, Y. C., Tzeng, T. T., Sun, Y. W. and Wung, B. S. 2008. Cinnamaldehyde inhibits the tumor necrosis factor-alpha-induced expression of cell adhesion molecules in endothelial cells by suppressing NF-kappaB activation: effects upon IkappaB and Nrf2. *Toxicol. Appl. Pharm.* 229: 161-171.
21. Stoyanova, E., Sandoval, S. B., Zuniga, L. A.,

- El-Yamani, N., Coll, E., Pastor, S., Reyes, J., Andres, E., Ballarin, J., Xamena, N. and Marcos, R. 2010. Oxidative DNA damage in chronic renal failure patients. *Nephrol. Dial. Transplant.* 25: 879-885.
22. Chen, J. and Shaikh, Z. A. 2009. Activation of Nrf2 by cadmium and its role in protection against cadmium-induced apoptosis in rat kidney cells. *Toxicol. Appl. Pharm.* 241: 81-89.
23. Alam, J., Killeen, E., Gong, P., Naquin, R., Hu, B., Stewart, D., Ingelfinger, J. R. and Nath, K. A. 2003. Heme activates the heme oxygenase-1 gene in renal epithelial cells by stabilizing Nrf2. *Am. J. Physiol. Renal Physiol.* 284: F743-752.
24. Applegate, L. A., Luscher, P. and Tyrrell, R. M. 1991. Induction of heme oxygenase: a general response to oxidant stress in cultured mammalian cells. *Cancer Res.* 51: 974-978.
25. Cosyns, J. P., Jadoul, M., Squifflet, J. P., De Plaen, J. F., Ferluga, D. and Ypersele de Strihou, C., 1994. Chinese herbs nephropathy: a clue to Balkan endemic nephropathy? *Kidney Int.* 45:1680-1688.
26. IARC, 2002. Summaries and Evaluation, *Aristolochia* species and aristolochic acids; International Agency for Research on Cancer: Lyon, France, Vol.82, pp 69-71.
27. Gold, L. S. and Slone, T. H. 2003. Aristolochic acid, an herbal carcinogen, sold on the Web after FDA alert. *N. Engl. J. Med.* 349, 1576-1577.
28. Chen, Y. Y., Chung, J. G., Wu, H. C., Bau, D. T., Wu, K. Y., Kao, S. T., Hsiang, C. Y., Ho, T. Y. and Chiang, S. Y. 2010. Aristolochic acid suppresses DNA repair and triggers oxidative DNA damage in human kidney proximal tubular cells. *Oncol Rep* 24: 141-153.
29. Hayes, J. D. and McLellan, L. I. 1999. Glutathione and glutathione-dependent enzymes represent a co-ordinately regulated defence against oxidative stress. *Free Radic. Res.* 31: 273-300.
30. Franco, R. and Cidlowski, J. A. 2006. SLCO/OATP-like transport of glutathione in FasL-induced apoptosis: glutathione efflux is coupled to an organic anion exchange and is necessary for the progression of the execution phase of apoptosis. *J. Biol. Chem.* 281: 29542-29557.
31. Russel, F. G., Masereeuw, R. and van Aabel, R. A. 2002. Molecular aspects of renal anionic drug transport. *Annu. Rev. Physiol.* 64: 563-594.
32. Liu, B. H., Wu, T. S., Yu, F. Y. and Su, C. C. 2007. Induction of oxidative stress response by the mycotoxin patulin in mammalian cells. *Toxicol. Sci.* 95: 340-347.
33. Woo, C. H., You, H. J., Cho, S. H., Eom, Y. W., Chun, J. S., Yoo, Y. J. and Kim, J. H. 2002. Leukotriene B(4) stimulates Rac-ERK cascade to generate reactive oxygen species that mediates chemotaxis. *J. Biol. Chem.* 277: 8572-8578.
34. Schmeiser, H. H., Janssen, J. W. G., Lyons, J., Scherf, H. R., Pfau, W., Buchmann, A., Bartram, C. R. and Wiessler, M. 1990. Aristolochic acid activates ras genes in rat tumors at deoxyadenosine residues. *Cancer Res.* 50: 5464-5469.
35. Schmeiser, H. H., Bieter, C. A., Wiessler, M., van Ypersele de Strihou, C. and Cosyns, J. P. 1996. Detection of DNA adducts formed by aristolochic acid in renal tissue from patients with Chinese Herbs Nephropathy. *Cancer Res.* 56: 2025-2028.